*J.Natn.Sci.Foundation Sri Lanka 2014 42 (1): 17-22*
DOI: http://dx.doi.org/10.4038/jnsfsr.v42i1.6674

**RESEARCH ARTICLE**

# Analysis of the behaviour of $SnO_2$ composites of ZnO and $TiO_2$ using impedance spectroscopy

**C.N. Nupearachchi*** **and V.P.S. Perera**
*Department of Physics, Faculty of Natural Sciences, The Open University of Sri Lanka, Nawala, Nugegoda.*

Revised: 24 May 2013; Accepted: 19 July 2013

**Abstract:** Composite semiconductor nanostructures will contribute in large measure for the future generation of cost effective optoelectronic devices. In order to advance the progress it is important to understand the mechanism of charge injection, transport and recombination in these systems. Impedance spectroscopy (IS) is a relatively old and powerful method for characterizing many of the electrical properties of materials and their interfaces. In this study, the impedance of composite porous films of $SnO_2$/ZnO and $SnO_2$/$TiO_2$ have been taken into consideration and their behaviour in composite films was analyzed using IS to describe the mechanism of charge carrier transportation.

The composites of $SnO_2$ and ZnO showed higher resistivity than their pure form and when $SnO_2$ : ZnO is in 1:1 ratio the resistivity of the composite film was the lowest ($7.6 \times 10^4$ kΩ m). When the percentage of $SnO_2$ is around 40 % and 90 % the resistivity of the films were higher where each of these cases could be explained by the depletion of electrons in the conduction band of $SnO_2$ and ZnO at the interface. In contrast to the $SnO_2$ and ZnO composite films, the minimum resistivity of $5.86 \times 10^5$ Ωm was obtained for $SnO_2$ and $TiO_2$ composite films when $SnO_2$ is 33 %, which is lower than when they are in pure form. This low resistivity of both composite films is possibly attributed to the formation of a super structure in the composites where the electrons transport ballistically in mini bands.

**Keywords:** Composite films, dye sensitized solar cells, impedance spectroscopy.

## INTRODUCTION

Composite materials sometimes exhibit rather unusual characteristics that are not prominent in pure materials and they could lead to novel applications and enhancements in existing devices. One of the fields that has remarkably developed during the past few years by the application of composite materials is the technology in dye sensitized photo electrochemical cells (PECs) where oxides of composite nanocrystalline semiconductor materials replaced the photo electrodes of PECs based on nanocrystalline $TiO_2$ (Tennakone *et al.,* 1999 ; Kitiyanan *et al.*, 2005; Hamann *et al.*, 2008; Nho & Cuong, 2008). Tennakone *et al.* (1999) had achieved a dramatic enhancement in the conversion efficiency of dye sensitized solar cells (DSSCs) with the application of mixed $SnO_2$ and ZnO semiconductor particles in the working electrode. An equally important issue in this development is to understand the mechanism of charge injection transport and recombination in these systems (Bisquert, 2002). However, the revelation of the enhancement mechanism is not completely explored. Yet, it can lead to further improvements of conversion efficiency and may contribute to the progress of future generation photovoltaic devices and applications in many other fields.

Intensive work in DSSC research has been devoted to the synthetic chemistry, structural and photovoltaic characterization of mesoporous nano crystalline $TiO_2$ materials and $TiO_2$ based DSSCs, which give a photo conversion efficiency of nearly 10 % (Grätzel, 2003). In contrast, other metal oxide semiconductors have gained less attention although they satisfy the necessary photo electrochemical properties similar to $TiO_2$. In fact $SnO_2$ has at least two advantageous features compared to $TiO_2$ for the application in DSSCs. Its higher electron mobility than $TiO_2$ suggests a faster transport of photo induced electrons by diffusion in $SnO_2$ than in $TiO_2$ and its larger

* Corresponding author (chathunilnupe@gmail.com)

band gap (3.8 eV) than the anatase phase of $TiO_2$ would create fewer oxidative holes in the valence band, so as to facilitate the long term stability of DSSCs (Qian *et al.*, 2009). However, $SnO_2$ based DSSCs were developed with less success and the conversion efficiencies of $SnO_2$ photo electrodes reported so far are much lower than those of $TiO_2$ (Chappel & Zaban, 2002).

In this study, the impedance of composite porous films deposited on conducting tin oxide (CTO) glass has been taken into consideration. A series of composite films were made with different mass percentages of $SnO_2$/ZnO and $SnO_2$/$TiO_2$. Impedance spectroscopy was used as the measuring tool in their characterization.

## METHODS AND MATERIALS

A series of nanocrystalline composite films of $SnO_2$ were prepared for different mass percentages of $SnO_2$/ZnO and $SnO_2$/$TiO_2$ while keeping the total mass at 0.5 g. Films (1 cm × 1 cm) of thickness 10 μm were prepared using doctor blade method on conducting tin oxide (CTO) glass plates (15 $\Omega cm^{-2}$), by grinding $SnO_2$ and ZnO (or $TiO_2$) powder with acetic acid and Triton X-100 in ethyl alcohol. These films were sintered at 450 $^0$C in a furnace for 30 min.

Complex plane impedance spectra of these films were measured by Solartron 1260 frequency response analyzer using SMART software, which is provided with the instrument. Sweeps were carried out for different mass percentages of $SnO_2$/ZnO and $SnO_2$/$TiO_2$ films coated on CTO glass with Pt sputtered glass plate as the counter electrode by setting the AC level at 100 mV in the frequency range of 1 MHz - 1 Hz while measuring the impedance in 1.0 s integrations.

## RESULTS AND DISCUSSION

A characteristic Nyquist plot of semi circular shape was observed for all the mass ratios of composites of $SnO_2$/ZnO and $SnO_2$/$TiO_2$ where some of them are shown in Figure 1 (a) and (b), respectively. Subsequently, to find the equivalent circuit and the significance of the different components the results were compared with a theoretical model. From the given impedance spectrum, the resistances and capacitance values of components in the equivalent circuit given in Figure 2 were calculated. The composites of $SnO_2$/ZnO and $SnO_2$/$TiO_2$ films deposited on CTO glass model a cell where the contact resistance ($Z_1$) of the CTO glass and the oxide semiconductors is in series with the parallel combination of capacitance (C) and resistance of the composite film ($Z_2$) as shown in Figure 2.

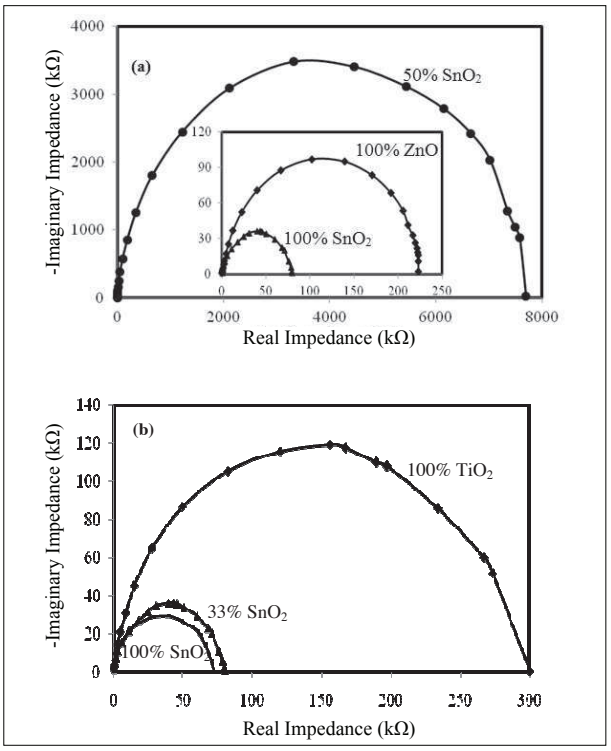


**Figure 1:** Nyquist plot of composite films made from (a) $SnO_2$ / ZnO and (b) $SnO_2$ / $TiO_2$

The values of the above parameters were found with the proper interpretation of the Nyquist plots using SMART software. For example, the capacitance was determined by examination of the maximum data point of the curve in the imaginary axis. The lowest intercept point of the curve with real axis gave a value for $Z_1$ and the second intercept gave the value of total resistance $Z_1$ and $Z_2$.

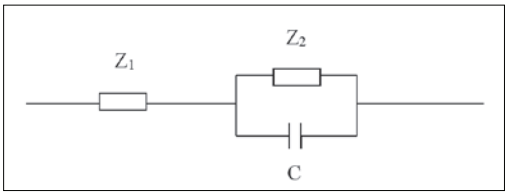


**Figure 2**: The equivalent circuit for composite $SnO_2$/ ZnO and $SnO_2$ / $TiO_2$ films

The average $Z_1$ value did not vary significantly in all compositions of $SnO_2$/ZnO and $SnO_2$/$TiO_2$ because it represents the contact resistance of the CTO glass with the composites, which was found to be around 486 Ω and 665 Ω, respectively.

However, the average $Z_2$ value, which is the parallel resistance of the films varied dramatically while altering the composition. The observation can be explained as follows for $SnO_2$/ZnO composite films. Since both the $SnO_2$ and ZnO are n-type semiconductors, their

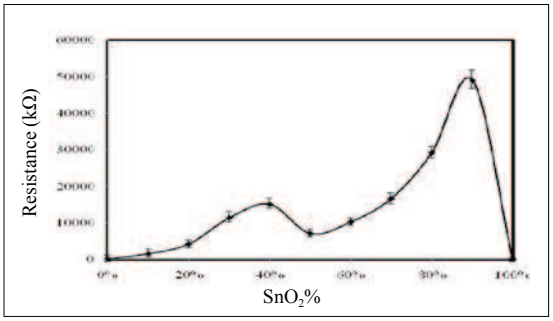


**Figure 3**: Plot of $Z_2$ vs $SnO_2$% (by weight) for $SnO_2$ and ZnO composite films

resistances are at low values when they are in pure form compared to other mixing ratios. In Figure 3, two peaks can be observed with minima at 50 % of $SnO_2$. The peaks correspond to an introduction of 40 % and 90 % of $SnO_2$ in the composite film. When we consider the first peak, the majority is ZnO particles (~ 60 % of the composite). Due to the space charge layer produced on ZnO by the depletion of electrons to $SnO_2$ particles (Zheng *et al.*, 2009; Uddin *et al.*, 2012), the conduction band is bent as shown in Figure 4(a).

In a single isolated $SnO_2$ or ZnO particle, band bending could not be observed because the particle size of both materials is less than 200 nm, where the depletion layer is generally spread out to 1 µm.

Figure 5 shows the scanning electron micrographs of (a) 100 % $SnO_2$ and (b) 50 % $SnO_2$ of $SnO_2$/ZnO composite films from which the particle sizes could be estimated. When the majority is $SnO_2$ particles as in

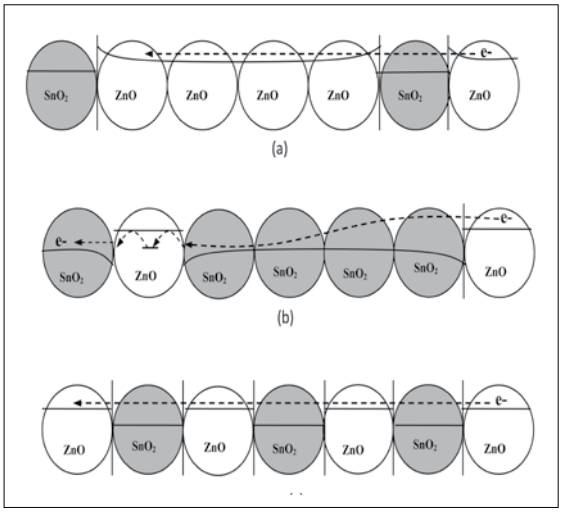


**Figure 4**: The mechanisms of electron transport in $SnO_2$ and ZnO composites at different mixing ratios (a) 40 % $SnO_2$ (b) 90 % $SnO_2$ and (c) 50 % $SnO_2$

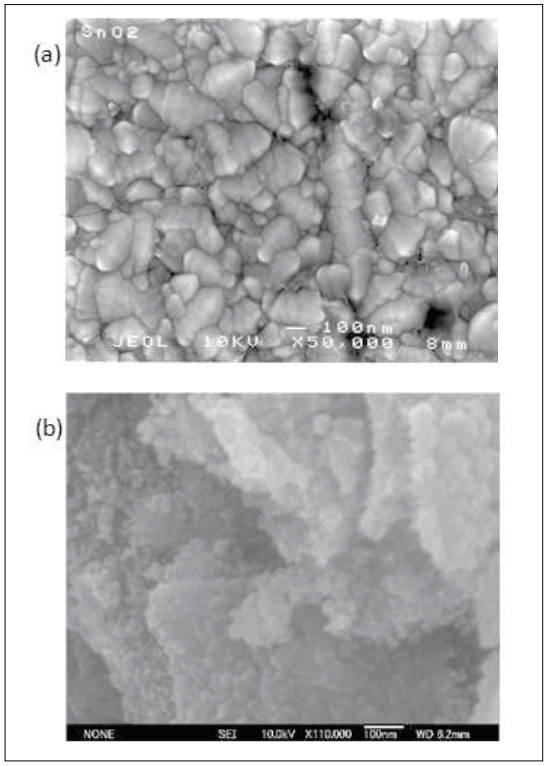


**Figure 5:** Scanning electron micrographs of (a) 100 % $SnO_2$ and (b) 50 % $SnO_2$ of $SnO_2$/ZnO composite films

Figure 4(b), the electrons may travel through several $SnO_2$ particles to meet a ZnO particle, which relaxes to the conduction band edge of $SnO_2$ on its way. Now the electron has a lower energy than the conduction band of ZnO. The only possible path for the electron to travel through the ZnO particle is hopping through the shallow traps in the ZnO particles, which will increase the resistance very much. A very high resistivity of the second peak at the composition of 90 % of $SnO_2$ is attributed to this reason. When both materials are in 1:1 ratio, transferring electrons have a less tendency to fall into the conduction band edge of the neighbouring $SnO_2$ particles. Here the electrons travel from one ZnO particle to another, tunnelling through the conduction band of $SnO_2$ particles as shown in Figure 4(c). Therefore in this situation, resistance of the film decreases to the minimum.

The results of this study correlates with the previous results of fabrication of dye-sensitized solar cells with composite of $SnO_2$ and ZnO (Kumara *et al.*, 2003). In the study the authors have clearly reported that the solar cells made with the 1:1 ratio of $SnO_2$ and ZnO has the highest efficiency.

In contrast to the $SnO_2$/ZnO composite films, the $Z_2$ value rapidly decreased in the composite film of

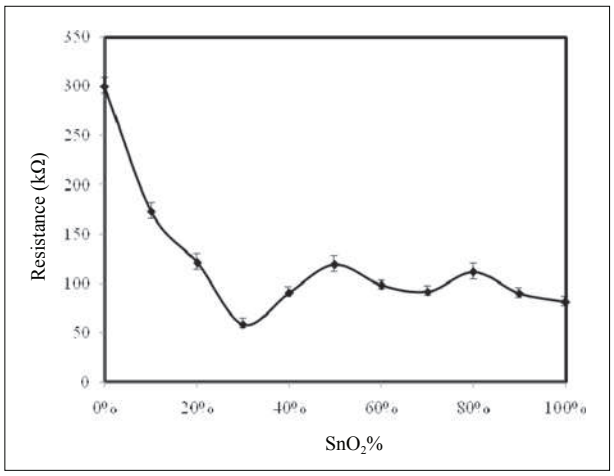


**Figure 6:** Plot of $Z_2$ *vs* $SnO_2$ % (by weight) for $SnO_2$ and $TiO_2$ composite films

$SnO_2/TiO_2$ while altering the composition (Figure 6). The wavy nature of the variation of impedance with the composition of the film is an interesting observation made in this study.

The average particle size of $TiO_2$ (Degussa P-25) and $SnO_2$ used in this study has been estimated with the particle size analyzer and scanning electron micrographs (SEM) and are in the order of 10 nm and 200 nm, respectively. Therefore at the preparation of the films, small $TiO_2$ particles tend to deposit on large $SnO_2$ particles, making a shell around it.

The thickness, $T$ of a shell around a core particle of average radius $r$ of this nature can be estimated using the formula

$$T = \frac{r}{3} \times \frac{W_S \rho_S}{W_C \rho_C} \quad ...(1)$$

where $W_S$: weight of shell material, $W_C$: weight of core material, $\rho_S$: density of shell material and $\rho_C$: density of core material (Bandaranayake *et al*., 2004).

The thickness can also be related to the roughness factor $R$ by the relation

$$T = \frac{W_C}{\rho_S R A} \quad ...(2)$$

where $A$ is the surface area of the film.

The thicknesses of the $TiO_2$ shell calculated using the above formula at the points which gave maximum and minimum resistivity of the film at different compositions is given in Table 1. In these calculations the density of $TiO_2$ and $SnO_2$ is taken as $4.23 \times 10^3$ kg $m^{-3}$ and $6.25 \times 10^3$ kg $m^{-3}$, respectively. The number of $TiO_2$ particles, $N$ that resides in between two consecutive $SnO_2$ particles in the composite is also estimated with the knowledge of the thickness of $TiO_2$ shell and the particle size of $TiO_2$ considering $r >> T$.

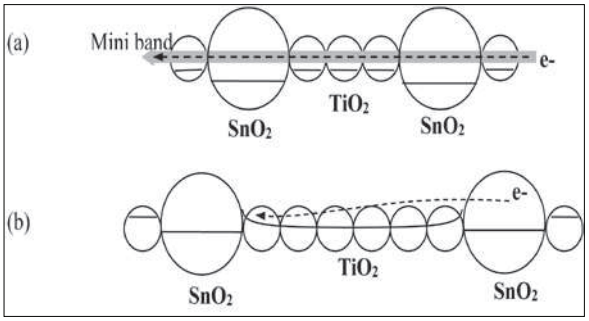


**Figure 7:** Electron transport in (a) mini bands and (b) hetero structures of $SnO_2$ and $TiO_2$ composites

The resistivity of pure $SnO_2$ ($0.9 \times 10^6$ Ωm) is very much less compared to the resistivity of pure $TiO_2$ ($3.0 \times 10^6$ Ωm) as evident from Figure 6. It also requires at least 20 % of $TiO_2$ in the composite film for monolayer coverage of $SnO_2$ particle according to Table 1. Therefore when the direct contacts of $SnO_2$ particles are forbidden by the inclusion of high resistive $TiO_2$ particles in between $SnO_2$ particles, it is obvious that the resistivity of the composite increases. This was prominent above 20 % of $TiO_2$ in the composite film. It is not clear why the resistivity decreases at 65 % and increases again at 50 % of $SnO_2$ in the composite film. This ambiguous behaviour has to be studied further to explain it meaningfully. The important finding of this study is that the resistivity of the composite film becomes lesser than the resistivity of both individuals when the film consists of 33 % of $SnO_2$. In this composition the average number of $TiO_2$ particles in between two $SnO_2$ particles is found to be 8. This kind of reduction of resistivity in a composite nanostructure

**Table 1:** Thickness of $TiO_2$ shell on $SnO_2$ particles and average number of $TiO_2$ particles resides in between two $SnO_2$ particles at different $SnO_2$ % of the composite films.

| $SnO_2$ % | 33 % | 50 % | 65 % | 80 % |
|---|---|---|---|---|
| T (nm) | 41.19 | 20.28 | 10.14 | 5.07 |
| N | 8 | 4 | 2 | 1 |

could only happen due to the formation of a super structure where electrons move ballistically (Figure 7a). The electron confining Bohr radius, $\alpha$ of a nanoparticle is given by

$$\alpha = \frac{\hbar}{(2m^* E)^{1/2}} \quad ...(3)$$

where $m^*$ is the electron effective mass.

The formation of a super structure with $SnO_2$ and $TiO_2$ seems possible, when the effective mass of electrons in $SnO_2$ and $TiO_2$ are considered, which are $0.1m_e$ and $10m_e$, respectively ($m_e$: rest mass of electron). The small effective mass of electrons in $SnO_2$ makes a longer length for electron confinement in $SnO_2$. Therefore, even 200 nm particles of $SnO_2$ could contribute to form a super structure in this composite film. On the other hand although the calculations indicate that there are 8 particles of $TiO_2$ in between two $SnO_2$ particles at this composition, in practice, it can vary from place to place.

Therefore the reason for the other compositions greater than 33 % of $SnO_2$ are unable to work as super structures is possibly because of the direct contacts of $SnO_2$ at high $SnO_2$ percentage levels, which do not support the formation of super structures. When the $SnO_2$ composition further reduces, the super structure disappears and band bending occurs in the $TiO_2$ phase (Figure 7b). At this stage a rapid increment of the resistivity of the composite could be observed as seen in Figure 6.

## CONCLUSION

The composites made by mixing $SnO_2$ and ZnO particles showed a high resistivity compared to each of them in pure form. However, compared to other mixing ratios, when $SnO_2$ and ZnO are in 1:1 ratio the resistivity of the composite film was the lowest ($7.6 \times 10^4$ kΩm). Again when the percentage of $SnO_2$ is around 40 % and 90 % the resistivity of the films were higher. Each of these cases can be explained by the depletion of electrons in the conduction band of $SnO_2$ and ZnO at the interface and the formation of a space charge layer. The analysis of impedance spectroscopic measurements of $SnO_2$ and ZnO composite films showed that the suggested approach is capable of describing the optimum mixing ratio of 1:1 in a frequency resolved measurement domain.

In contrast to the $SnO_2$ and ZnO composite films, a minimum resistivity of $5.86 \times 10^5$ Ωm was obtained for $SnO_2$ and $TiO_2$ composite films when the percentage of $SnO_2$ is 33 %, which is lower than when they are in pure form. This low resistivity of the film is possibly attributed to the formation of a super structure in the composite where the electrons transport ballistically in mini bands. These structures could be preliminary tested in the future for optoelectronic devices such as solar cells to optimize their efficiencies.

## REFERENCES


1. Bandaranayake K.M.P., Seneviratne M.K.I., Weligamuwa P.M.G.M. & Tennakone K. (2004). Dye sensitized solar cells made from nanocrystalline $TiO_2$ films coated with outer layers of different oxide materials. *Coordination Chemistry Reviews* **248**: 1277 − 1281. DOI: http://dx.doi.org/10.1016/j.ccr.2004.03.024
2. Bisquert J. (2002). Theory of the impedance of electron diffusion and recombination in a thin layer. *The Journal of Physical Chemistry B* **106**: 325 − 333. DOI: http://dx.doi.org/10.1021/jp011941g
3. Chappel S. & Zaban A. (2002). Nanoporous $SnO_2$ electrodes for dye sensitized solar cells: improved cell performance by the synthesis of 18nm $SnO_2$ colloids. *Solar Energy Materials and Solar cells* **71**: 141 − 152.
4. Grätzel M. (2003). Dye sensitized solar cells. *Journal of Photochemistry and Photobiology C: Photochemistry Reviews* **4**: 145 − 153.
5. Hamann T.W., Martinson A.B.F., Elam J.W., Pellin M.J. & Hupp J.T. (2008). Aerogel templated ZnO dye sensitized solar cells. *Advanced Materials* **20**: 1560 − 1564. DOI: http://dx.doi.org/10.1002/adma.200702781
6. Kitiyanan A., Pavasupree S., Kato T., Suzuki Y. & Yoshikawa S. (2005). $TiO_2$- $ZrO_2$ mixed metal oxide electrode for a dye sensitized solar cell. *Asian Journal on Energy and Environment* **6**(3): 165 − 174.
7. Kumara G.R.R.A., Tennakone K., Kottegode I.R.M., Bandaranayake P.K.M., Knno A., Okuya M., Kaneko S. & Murakami K. (2003). Efficient dye-sensitized photoelectrochemical cells made from nanocrystalline tin (IV) oxide- zinc oxide composite films. *Semiconductor Science and Technology* **18**: 312 − 318. DOI: http://dx.doi.org/10.1088/0268-1242/18/4/321
8. Nho P.V. & Cuong T.K. (2008). Preparation and characterization of nanocomposite $TiO_2$/ $SnO_2$ films. *VNU Journal of Science, Mathematics-Physics* **24**: 42 − 46.
9. Qian J., Liu P., Xiao Y., Jiang Y., Cao Y., Ai X. & Yang H. (2009). $TiO_2$ coated multilayered $SnO_2$ hollow microspheres for dye sensitized solar cells. *Advanced Materials* **21**: 3663 − 3667. DOI: http://dx.doi.org/10.1002/adma.200900525
10. Tennakone K., Kumara G.R.R.A., Kottegoda I.R.M.

& Perera V.P.S. (1999). An efficient dye-sensitized photoelectrochemical cell made from oxides of tin and zinc. *Chemical Communications* **1**: 15 − 16.
DOI: http://dx.doi.org/10.1039/a806801a

11. Uddin M.T., Nicolas Y., Olivier C., Toupance T., Servant L., Müller M.M., Kleebe H.J., Ziegler J. & Jaegermann W. (2012). Nanostructured $SnO_2$-ZnO heterojunction photocatalysts showing enhanced photocatalytic activity for the degradation of organic dyes. *Inorganic Chemistry Communications* **51**: 7764 − 7773.
DOI: http://dx.doi.org/10.1021/ic300794j
12. Zheng L., Zheng Y., Chen C., Zhan Y., Lin X., Zheng Q., Wel K. & Zhu J. (2009). Network structured $SnO_2$/ZnO heterojunction nanocatalyst with high photocatalytic activity. *Inorganic Chemistry Communications* **48**: 1819 − 1825.
DOI: http://dx.doi.org/10.1021/ic802293p